Analytical and Bioanalytical Chemistry (2022) 414:3397–3410
https://doi.org/10.1007/s00216-022-03958-z

RESEARCH PAPER

An integrated ICP-MS-based analytical approach to fractionate and characterize ionic and nanoparticulate Ce species

Yingyan Huang[1] · Judy Tsz-Shan Lum[1] · Kelvin Sze-Yin Leung[1,2]

Received: 17 October 2021 / Revised: 26 January 2022 / Accepted: 2 February 2022 / Published online: 7 February 2022

Abstract

Cerium dioxide nanoparticles (CeO_2 NPs) are widely used in various fields, leading to concern about their effect on human health. When conducting in vivo investigations of CeO_2 NPs, the challenge is to fractionate ionic Ce and CeO_2 NPs and to characterize CeO_2 NPs without changing their properties/state. To meet this challenge, we developed an integrated inductively coupled plasma-mass spectrometry (ICP-MS)-based analytical approach in which ultrafiltration is used to fractionate ionic and nanoparticulate Ce species while CeO_2 NPs are characterized by single particle-ICP-MS (sp-ICP-MS). We used this technique to compare the effects of two sample pretreatment methods, alkaline and enzymatic pretreatments, on ionic Ce and CeO_2 NPs. Results showed that enzymatic pretreatment was more efficient in extracting ionic Ce or CeO_2 NPs from animal tissues. Moreover, results further showed that the properties/states of all ionic and nanoparticulate Ce species were well preserved. The rates of recovery of both species were over 85%; the size distribution of CeO_2 NPs was comparable to that of original NPs. We then applied this analytical approach, including the enzymatic pretreatment and ICP-MS-based analytical techniques, to investigate the bioaccumulation and biotransformation of CeO_2 NPs in mice. It was found that the thymus acts as a "holding station" in CeO_2 NP translocation in vivo. CeO_2 NP biotransformation was reported to be organ-specific. This is the first study to evaluate the impact of enzymatic and alkaline pretreatment on Ce species, namely ionic Ce and CeO_2 NPs. This integrated ICP-MS-based analytical approach enables us to conduct in vivo biotransformation investigations of CeO_2 NPs.

Keywords Cerium dioxide nanoparticles · Inductively coupled plasma-mass spectrometry · Fractionation · Biotransformation · Dissolution · Size characterization

Introduction

Cerium dioxide nanoparticles (CeO_2 NPs), as one of the most widely used engineered nanomaterials, have been prioritized for environmental characterization and assessment by the Organization for Economic Cooperation and Development (OECD). The market volume of CeO_2 NPs was estimated to be 9.1 kilotons in 2016 [1], and usage is expected to increase due to their wide applications as catalysts, abrasive agents, and polishing agents [1, 2]. The downside of broad applications of CeO_2 NPs is that NPs are leaking into the environment. There is increasing evidence of CeO_2 NPs' occurrence in rivers [3–5] and of anthropogenic Ce in air/urban dust [6] as well as in sediment/sewage sludge [7, 8]. Furthermore, the possibility of CeO_2 NPs entering the food chain has been shown [9, 10]. Therefore, humans are being exposed to CeO_2 NPs through various routes. This arouses concern. Hence, a better understanding of CeO_2 NP biological fate is necessary to protect the environment and human health.

After uptake by mammals, CeO_2 NPs may interact with biomolecules/chemicals, leading to biotransformation (e.g., dissolution of NPs and aggregation/agglomeration) [11]. For example, CeO_2 NPs may dissolve ionic Ce or change in size after their uptake. In order to investigate the biological fate of CeO_2 NPs in organisms, it is critical to first ensure release of the NPs and possibly dissolved Ce from the animal tissues. This requires appropriate sample preparation and analytical methods to separate both ionic and nanoparticulate Ce species followed by characterization/quantification.

✉ Kelvin Sze-Yin Leung
s9362284@hkbu.edu.hk

[1] Department of Chemistry, Hong Kong Baptist University, Kowloon Tong, Hong Kong Special Administrative Region, People's Republic of China

[2] HKBU Institute of Research and Continuing Education, Shenzhen Virtual University Park, Shenzhen, People's Republic of China

Previous studies have reported that ionic Ce is more toxic than CeO_2 NPs at a similar concentration level [12, 13], possibly due to the Ce^{3+}-induced conformational changes to catalase [14]. Furthermore, CeO_2 NP size, another physicochemical property of NPs, also affects the toxicity of NPs [12, 15]. In other words, the toxicity of CeO_2 NPs is closely related to the Ce species and NP size. To address the biotransformation (i.e., dissolution and size transformation in this study) of CeO_2 NPs in vivo, firstly, Ce species and size of CeO_2 NPs are required to be well preserved after their release from animal tissues; secondly, the analytical methods should be able to differentiate the Ce species as well as characterize the NP size after releasing both Ce species from animal tissues. Finding a sample preparation method that does not alter properties of NPs or dissolved species during the extraction or separation of Ce species from animal tissues is a challenge for in vivo investigations of CeO_2 NPs. Previous studies have applied different methods to extract NPs from animal tissues, such as alkaline pretreatment using tetramethylammonium hydroxide (TMAH) and enzymatic pretreatment using proteinase K [16–19]. However, little attention has been given to evaluate the effect of sample preparation methods on ionic Ce and CeO_2 NPs. Moreover, most studies focused on the characterization of CeO_2 NPs but neglected the possible dissolution of CeO_2 NPs [17, 18].

Worse still, limitations of analytical techniques in characterizing and quantifying CeO_2 NPs as well as the possibility that dissolved species, results of biotransformation, may occur in biological matrices complicate the in-depth investigation of their biological fate. It is technically especially difficult to quantify dissolved NPs at low particle concentrations [20]. For in vivo investigation of NPs, the conventional analytical techniques for NP characterization, such as dynamic light scattering (DLS) and nanoparticle tracking analysis (NTA), are not suitable due to their relatively high detection limit. Microscopy techniques, such as transmission electron microscopy (TEM) and scanning electron microscopy (SEM), are limited to the local characterization of NPs in tissue and cannot provide quantitative information of NPs, such as their size distribution and particle number concentration. Among various techniques for NP investigation, inductively coupled plasma-mass spectrometry (ICP-MS) is promising. When appropriate separation system is hyphenated to ICP-MS, it shows good performance in both qualitative and quantitative investigations of metal-containing NPs [21]. Size exclusion chromatography (SEC) — it is showing great potential for fractionating and quantifying (nano) particulate and ionic Ce species in environmental water samples [22]. Multi-method approach, including extraction, (ultra)filtration and asymmetric flow field flow fractionation (AF4)-ICP-MS, was applied to separate and quantify ionic Ce species dissolved from CeO_2 NPs in surface waters [23], leaching solution [24], Luria–Bertani (LB) medium [25], algae growth media [26], and the enzymatic digestate of plant tissue [27]. However, these techniques are limited to the CeO_2 NPs suspended in environmentally or botanically relevant samples, and none have been developed to fractionate the (nano)particulate and dissolved Ce species in animal samples. This lack of methodology is a major factor for our lack of understanding of CeO_2 NP biotransformation in vivo.

For NPs suspended in an aqueous solution, they can be introduced and analyzed directly by ICP-MS operated in single particle mode (sp-ICP-MS). This technique can provide size distribution, mass concentration, and particle number concentration of NPs simultaneously at very low concentration levels. Although the simple sample preparation method (i.e., dilution of the aqueous samples) entails the risk of possible severe matrix effect on accuracy, precision, and sensitivity in sp-ICP-MS analysis, our previous work has shown that sp-ICP-MS combined with internal standardization accurately characterizes CeO_2 NPs in complex biological matrices [28]. Zhang et al. [27] have utilized Amicon® Centrifugal filter to separate dissolved Ce in a CeO_2 NP suspension. The success of these studies demonstrates that there is a potential to use ICP-MS-based techniques to investigate the biotransformation of CeO_2 NPs, particularly their dissolution and size transformation in vivo. This information will give us a quantitative and more comprehensive understanding of their fate after their uptake by organisms.

In this work, we aimed to develop a multistep ICP-MS-based analytical approach for extraction of nanoparticulate as well as ionic Ce species from animal tissue, quantification of Ce species, and then characterization of CeO_2 NPs. The fractionation of ionic and nanoparticulate species was achieved using ultra-centrifugal units. Conventional ICP-MS was used to quantify different Ce species and the characterization of CeO_2 NPs was completed by sp-ICP-MS. With this integrated ICP-MS-based analytical approach, a comparison of alkaline and enzymatic pretreatment was done. This integrated analytical approach then was applied to investigate the in vivo biotransformation of CeO_2 NPs.

Materials and methods

Chemicals and materials

CeO_2 NPs dispersed in aqueous solution (40 wt%, 30–50 nm) were purchased from US Research Nanomaterials, Inc. (TX, USA). Standard gold nanoparticles (AuNPs) with a nominal diameter of 60 nm, which was used to determine the transport efficiency in sp-ICP-MS analysis, were from BBI Solutions (Cardiff, UK). $Ce(NO_3)_3{\cdot}6H_2O$ (REacton®, 99.99% (REO)) for method validation was obtained from Alfa Aesar, Thermo Fisher Scientific, UK. The standards of ionic Ce, gold (Au), and rhodium (Rh) at 1000 mg/L were obtained

from VHG Lab (Teddington, Middlesex, UK). TMAH (25% v/v) used for alkaline pretreatment was purchased from Alfa Aesar (Ward Hill, MA, USA). Chemicals for preparing the enzymatic solution, including proteinase K from Tritirachium album lyophilized powder (BioUltra, ≥ 99.0%), ethylenediaminetetraacetic acid (EDTA) dipotassium salt dihydrate (≥ 98%), sodium dodecyl sulfate (SDS, BioUltra, ≥ 99.0%), and tris(hydroxymethyl)aminomethane (Tris) (ACS reagent, ≥ 99.8%), were purchased from Sigma-Aldrich (St. Louis, MO, USA). Ca^{2+}- and Mg^{2+}-free Dulbecco's phosphate buffered saline (DPBS, pH 7.4) was obtained from Gibco, Life Technologies (Carlsbad, CA, USA). Trace-metal grade concentrated HNO_3 and concentrated HCl as well as 30% stabilized H_2O_2 were purchased from VWR Chemicals (Poole, UK). Ultrapure water (18.2 MΩ cm at 25 °C) was obtained from a Milli-Q® Reference Water Purification System (Millipore, USA).

Characterization of CeO_2 NPs

The CeO_2 NPs without any surface modification were diluted with ultrapure water and were ultrasonicated to ensure the homogeneous distribution prior to usage. They were fully characterized by TEM (JEOL 2010F, Japan), DLS (Zetasizer Nano-S system, Malvern, UK), and X-ray photoelectron spectroscopy (XPS, SKL-12 spectrometer modified with VG CLAM 4 multichannel hemispherical analyzer) in our previous study [29]. The particle size of commercial CeO_2 NPs was shown to be in the range of 30–50 nm by TEM, and most particles are round, which corresponds to the description provided by the manufacturer. The DLS measurement showed that the hydrodynamic size of CeO_2 NPs in ultrapure water was 152.7 ± 1.6 nm and the average zeta potential was − 53.2 ± 1.0 mV. The XPS result showed that Ce^{4+} dominates on the surface of CeO_2 NPs.

Animals and experimental design

Thirty-two 8-week-old female ICR mice were purchased from Laboratory Animal Service Centre, The Chinese University of Hong Kong (Hong Kong, China). The animal study was performed in compliance with The Hong Kong Code of Practice for Care and Use of Animals for Experimental Purposes [30]. Prior to the experimental treatment, they were acclimated in the animal room environment with a 12 h light/dark cycle (temperature of 22 ± 1 °C, relative humidity of 50–70%) and they had free access to food and water. After 5-day acclimation, they were randomly divided into vehicle control groups ($n = 3$) and experimental groups ($n = 5$). The experimental groups were intraperitoneally administered with 1.23 mg CeO_2 NPs (as 1 mg Ce)/kg body weight dispersed in 200 µL DPBS, while the vehicle control groups were treated with DPBS with the same volume. All mice were weighed weekly to monitor their health. After the single intraperitoneal administration, mice were sacrificed on 1st, 7th, 28th, and 90th day(s) by cervical dislocation.

After the mice were terminated by cervical dislocation, livers, spleens, thymuses, and kidneys were removed after dissection. Parts of the liver tissues were frozen at − 80 °C for biochemical assays. The rest of the liver tissues, spleens, thymuses, and kidneys were lyophilized and stored at − 20 °C for CeO_2 NP biodistribution and biotransformation analysis.

Development of an integrated ICP-MS-based analytical approach

A schematic diagram of the integrated ICP-MS-based analytical approach is shown in Fig. 1. Briefly, the total Ce concentration in samples was determined by conventional ICP-MS after the microwave-assisted acid digestion with enzymatic or alkaline pretreatment. The ionic Ce was separated by ultrafiltration and quantified by conventional ICP-MS. The characterization of CeO_2 NPs was completed by sp-ICP-MS after simple dilution of the pretreated samples.

Spiking experiments

Since no reference material containing CeO_2 NPs or ionic Ce was available, the lyophilized ground liver tissue spiked with CeO_2 NPs or ionic Ce was used to compare the effect of enzymatic and alkaline pretreatment on the recovery of each species. In addition, evaluation of the integrated ICP-MS-based analytical approach with suitable sample pretreatment methods was also completed with the spiked tissue.

Comparison of sample preparation methods

In order to extract the Ce species from animal tissues, both alkaline and enzymatic pretreatments were evaluated and their effect on ionic Ce as well as CeO_2 NPs was compared. The alkaline pretreatment was developed based on a study where silver nanoparticles (AgNPs) were extracted from human placenta [19]. Briefly, 25% (v/v) TMAH solution was diluted to 20% with ultrapure water. Four milligrams of lyophilized tissue was weighed and digested with 2 mL of 20% TMAH solution. The samples were vortexed to mix thoroughly and left at room temperature overnight. The enzymatic solution was prepared by dissolving 0.2% (w/v) proteinase K, 0.8% EDTA (w/v), and 0.5% (w/v) SDS in 10 mM Tris–HCl buffer (pH 7.4). Four milligrams of lyophilized tissue was weighed and digested with 2 mL of enzyme solution (0.1 g of enzyme per g of lyophilized tissue). Samples were vortexed and then left in a water bath at 37 °C overnight.

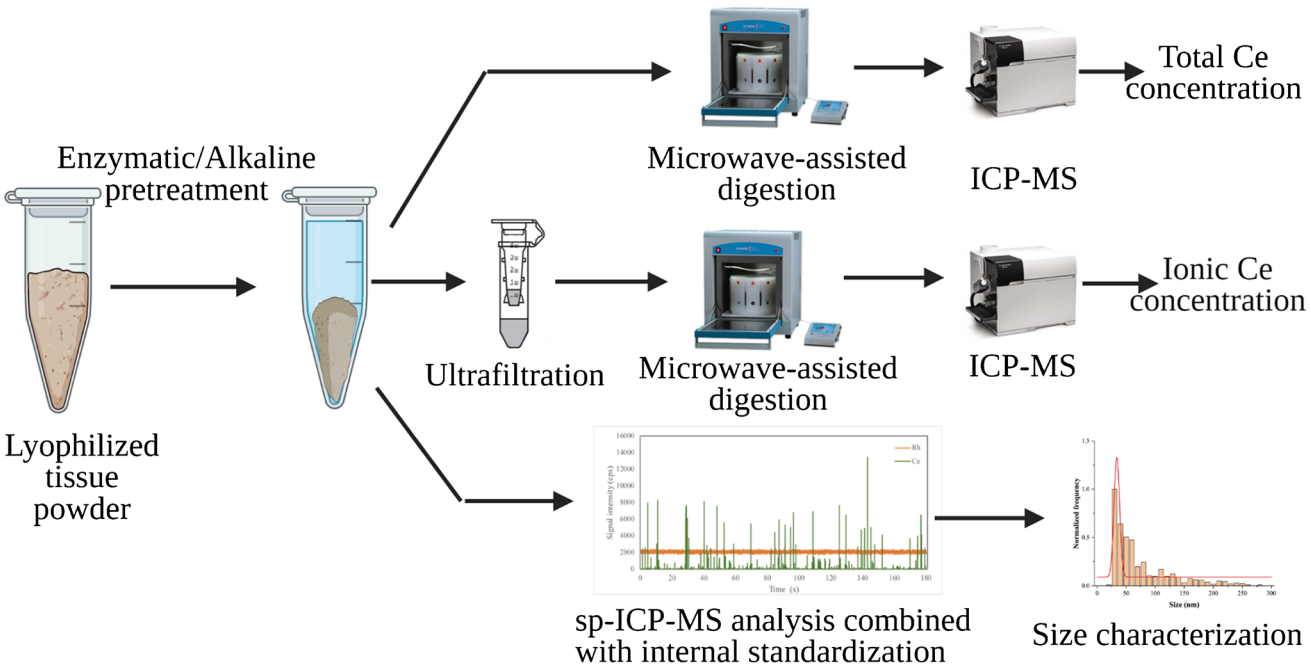

Fig. 1 Schematic diagram of the integrated ICP-MS-based analytical approach

Total mass concentration and ionic mass concentration

The sample solution right after the pretreatment was used for the total Ce (including CeO_2 NPs and ionic Ce) quantification. Four hundred microliters of the enzyme-digested solution was mineralized by mixing with 3 mL concentrated HNO_3 and 1 mL 30% H_2O_2 in a microwave digestion system (ETHOS-1 Advanced, Milestone S.r.l., Sorisole, Italy). Total Ce concentration (^{140}Ce) was determined using ICP-MS (7900 Agilent Technologies, Inc., CA, USA). The instrument settings are listed in Table 1.

The ionic Ce was separated by ultrafiltration. Briefly, 400 µL of a sample solution was passed through Amicon® 3 K cellulose filters (Merck, Darmstadt, Germany) pre-rinsed with ultrapure water. The filtrate, containing mainly the ionic Ce content, was collected after centrifugation (× 14,000 *g*, 22 °C, 30 min), and the ionic Ce was quantified by ICP-MS after microwave-assisted acid digestion as described above.

Table 1 Instrument settings for sp-ICP-MS and conventional ICP-MS analysis

Parameters	sp-ICP-MS	ICP-MS
RF power (W)	1400	1400
Plasma gas flow (L/min)	14.0	14.0
Auxiliary gas flow (L/min)	1.0	1.0
Carrier gas flow (L/min)	1.05	1.05
Cones	Nickel	Nickel
Nebulizer and spray chamber	Micromist, Scott-type double-pass (2 °C)	Micromist, Scott-type double-pass (2 °C)
Sample uptake rate (mL/min)	0.25–0.35 (determined weekly)	0.25–0.35
Analysis mode	Standard	Standard
Data acquisition mode	Time-resolved analysis (TRA)	Spectrum
Integration time	10 ms	-
Measurement duration	180 s (dual element monitoring, approximately 75 s for each mass)	-
Monitored elements	^{103}Rh, ^{140}Ce	^{140}Ce

Characterization of CeO_2 NPs using sp-ICP-MS

The Agilent 7900 ICP-MS operating in the time-resolved analysis (TRA) mode was used for the characterization of CeO_2 NPs. The detailed instrumental settings and data acquisition parameters are listed in Table 1. The transport efficiency, defined as the ratio of the amount of target analyte entering the plasma to the amount of analyte aspirated, was determined daily using the particle size method developed by Pace et al. [31], in which the AuNP standard with a nominal diameter of 60 nm was used as the reference material. The flow rate was determined weekly by measuring the time spent by the peristaltic pump to take up 1 mL of water. Prior to the sp-ICP-MS analysis, the alkali-pretreated or enzyme-pretreated sample solutions were diluted with ultrapure water. Based on the instrumental settings, flow rate, and the transport efficiency of ICP-MS, the appropriate particle number concentration for NP characterization was in the range of 6,000–12,000 particles/mL.

Considering that the concentration of CeO_2 NPs in tissue would be low in the real sample analysis, the dilution factors of the samples suited for sp-ICP-MS analysis may be small correspondingly. This would result in a pronounced matrix effect in sp-ICP-MS analysis. Therefore, the internal standardization developed in our previous work was applied in the sp-ICP-MS analysis for a more accurate characterization of NPs [28]. Briefly, the ionic rhodium (Rh) was used as the internal standard for the characterization of CeO_2 NP by sp-ICP-MS, and dual mass mode (i.e., detection of two masses in a single measurement run) was applied to monitor ^{140}Ce and ^{103}Rh. Prior to the sp-ICP-MS analysis, the samples were spiked with 1 µg/L ionic Rh. ^{140}Ce and ^{103}Rh were monitored in sp-ICP-MS using dual mass mode. The raw data were processed by Microsoft Excel to generate the mass concentrations, size distributions, and particle number concentrations. The calculations were based on the presumption that CeO_2 NPs are spherical, which corresponds to the TEM image of CeO_2 NPs.

Statistical analysis

Values are presented as mean ± standard deviation (SD). Statistical differences were determined using one-way analysis of variance (ANOVA) followed by Tukey post hoc multiple comparison test. Statistical differences were considered to be significant when $p < 0.05$ and was indicated with *.

Results and discussion

Integrated ICP-MS-based analytical approach for fractionation of Ce species in animal tissues

Comparison of alkaline and enzymatic pretreatment

Previous investigations of CeO_2 NPs in biological bodies have neglected the possibility of dissolution of CeO_2 NPs. As a result, the efficiency of extraction methods was evaluated merely in terms of their effect on NPs, while the performance of the sample preparation method on dissolved Ce species was ignored. To fill this knowledge gap, in this study, we compared the extraction efficiency of alkaline and enzymatic pretreatment towards both CeO_2 NPs and ionic Ce. Alkaline solubilization, commonly with TMAH, has been used to liberate AuNPs or AgNPs from animal tissues with good recovery [19, 32]. Similarly, enzymatic pretreatment, using proteinase to degrade proteins, was shown to be effective to extract AuNPs or AgNPs from animal tissues [19, 32, 33]. To simulate the possible low concentration of ionic Ce or CeO_2 NPs in animal tissue, the spiked ionic Ce concentration was 5 mg Ce/kg dry tissue and the CeO_2 NPs were spiked at a concentration of 4.06 mg Ce/kg dry tissue. Since no standard CeO_2 NPs were available, a suspension of CeO_2 NPs in ultrapure water was also prepared for CeO_2 NPs in sp-ICP-MS analysis for comparison.

In this integrated ICP-MS-based analytical approach, the ionic Ce in the medium was fractionated by ultrafiltration and quantified by conventional ICP-MS. The characterization of CeO_2 NPs was completed by sp-ICP-MS, in which internal standardization was applied to increase the accuracy.

Table 2 shows the recoveries of alkaline and enzymatic pretreatment. In terms of the extraction of ionic Ce, the low recovery (1.1 ± 1.0%) obtained after alkaline pretreatment indicated that ionic Ce might form precipitates in the TMAH-pretreated matrix. The result obtained by sp-ICP-MS further confirmed the presence of precipitates in the TMAH-pretreated matrix (Fig. S1). For enzymatic pretreatment, the recovery of ionic Ce achieved 89 ± 3%.

When extracting the CeO_2 NPs from animal tissues using proteinase K, less than 1% of the CeO_2 NPs was dissolved during the extraction process. In addition, the mass concentration recovery and the particle number recovery were over 90%, and the size distribution of CeO_2 NPs after extraction was comparable with those in ultrapure water by sp-ICP-MS (Fig. 2). These results demonstrated that enzymatic pretreatment does not alter the state of CeO_2 NPs; it would not cause dissolution or size aggregation of CeO_2 NPs. In terms of alkaline pretreatment, the dissolution test was comparable with the case of enzymatic pretreatment. However, the recovery of mass concentration and particle number in sp-ICP-MS analysis reached 114.8 ± 1.0% and 223 ± 23.7%, respectively. Worse still, the size distribution of CeO_2 NPs showed obvious left skew after alkaline pretreatment, indicating that the frequency of CeO_2 NPs with smaller diameter increased. The increased mass concentration and particle number concentration in TMAH-pretreated matrix suggested that the TMAH-pretreated matrix might have impact on the transport efficiency during the

Table 2 Recovery of ionic Ce and CeO_2 NPs in biological lyophilized tissue after enzymatic or alkaline pretreatment ($n=3$)

Pretreatment method	Spiked ionic Ce	Spiked CeO_2 NPs		
	Recovery of ionic Ce (%)	Dissolution of CeO_2 NPs (%)	Mass recovery of CeO_2 NPs in sp-ICP-MS[a] (%)	Particle number recovery in sp-ICP-MS[b] (%)
Enzymatic pretreatment	88.9 ± 3.1	0.81 ± 0.05	98.1 ± 9.2	91.8 ± 1.7
Alkaline pretreatment	1.1 ± 1.0	0.73 ± 0.08	114.8 ± 1.0	223 ± 22.7

[a]The mass recovery of CeO_2 NPs in sp-ICP-MS was calculated by the mass concentration obtained from sp-ICP-MS divided by that obtained through conventional ICP-MS after microwave-assisted digestion

[b]Particle number recovery of CeO_2 NPs after enzymatic or alkaline pretreatment was calculated and then compared with those suspended in ultrapure water

sp-ICP-MS analysis. To further address this problem, standard AuNPs were spiked in the TMAH-pretreated matrix (500-times diluted) and enzyme-pretreated matrix (500-times diluted), and the results obtained by sp-ICP-MS were compared with the case of AuNPs suspended in ultrapure water (Table 3). Internal standardization was also applied to correct for the matrix effect on signal intensity. The transport efficiency was determined to be 6.6 ± 0.1% in TMAH-pretreated matrix, which was significantly larger than that determined in ultrapure water. While for the enzyme-pretreated matrix, the determined transport efficiency was comparable with that in ultrapure water. This result demonstrated that the matrix after alkaline pretreatment would increase the transport efficiency at low dilution level. It is believed that the presence of TMAH and organic carbon species after sample preparation decreases the surface tension, resulting in smaller droplets generated in the nebulizer [34, 35]. Hence, the transport efficiency was increased in sp-ICP-MS measurement. Although more accurate transport efficiency can be obtained by matrix-matched determination, it requires tedious preparation steps and is not practicable in real sample analysis, where the dilution factor is not always consistent for each sample.

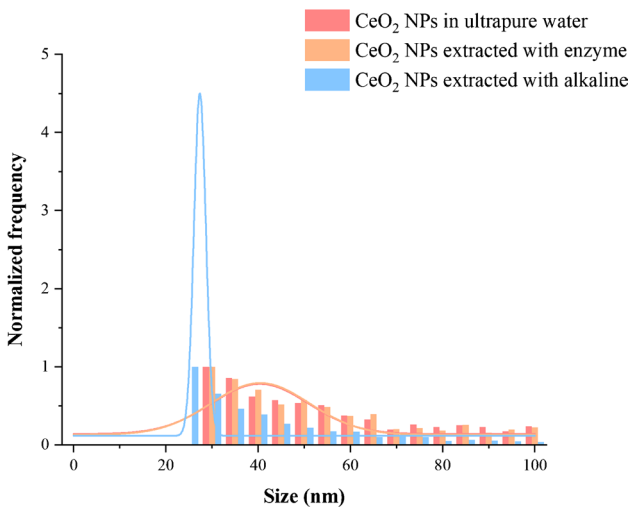

Fig. 2 Size distributions of CeO_2 NPs in ultrapure water and of CeO_2 NPs after extraction with TMAH and enzyme from animal tissues, which were obtained by sp-ICP-MS

Through the comparison of alkaline and enzymatic pretreatment, it was found that enzymatic pretreatment not only showed satisfactory recovery of both ionic Ce and CeO_2 NPs when extracting Ce species from animal tissues but also preserved the size of CeO_2 NPs.

Performance of the integrated ICP-MS-based analytical approach

Enzymatic pretreatment was proven to be more effective to release ionic Ce as well as CeO_2 NPs from biological system without altering the species or size of NPs. Through this integrated analytical approach, the total Ce concentration, ionic Ce concentration, and characterization of CeO_2 NPs were studied based on the same enzyme-pretreated solution, thereby reducing any variation that might be introduced. In order to evaluate the performance of the integrated ICP-MS-based analytical approach using enzymatic pretreatment for sample preparation, both ionic Ce and CeO_2 NPs were spiked in lyophilized tissue, at concentrations of 5 μg Ce/g tissue and 43 μg Ce/g tissue, respectively. The recoveries are shown in Table 4. A comparison of CeO_2 NP characterization is shown in Fig. 3 using both

Table 3 Transport efficiency determined by AuNPs suspended in ultrapure water and alkali-pretreated matrix (500-times diluted) using the particle size method ($n=3$)

Suspended medium	Transport efficiency (%)
Ultrapure water	5.6 ± 0.4
Enzyme-pretreated matrix	5.2 ± 0.6
Alkali-pretreated matrix	6.6 ± 0.1

Table 4 Recovery of mixed ionic Ce and CeO_2 NPs in biological lyophilized tissue extracted with enzymatic pretreatment and the LOQ of each step in the integrated ICP-MS-based analytical approach ($n=3$)

ICP-MS (for total Ce including ionic and nanoparticulate Ce)		Ultrafiltration (for ionic Ce)		sp-ICP-MS (for CeO_2 NPs)		
Mass recovery of total Ce (%)	LOQ (μg/g)	Mass recovery of ionic Ce (%)	LOQ (μg/g)	Mass recovery of CeO_2 NPs[a] (%)	Particle number recovery of CeO_2 NPs (%)	Size LOD (nm)
86.6 ± 1.8	0.005	90.2 ± 0.5	0.005	89.0 ± 3.5	94.8 ± 3.1	15

[a]Mass recovery was calculated as the mass concentration determined by sp-ICP-MS over the difference of total Ce concentration and ionic Ce concentration

sp-ICP-MS and TEM techniques: the size distribution of CeO_2 NPs was comparable with that in ultrapure water (Fig. 3a), and the TEM photographs of CeO_2 NPs after enzymatic pretreatment compared with the original CeO_2 NPs (Figs. 3b and c) further demonstrate that enzymatic pretreatment will not change the size of CeO_2 NPs.

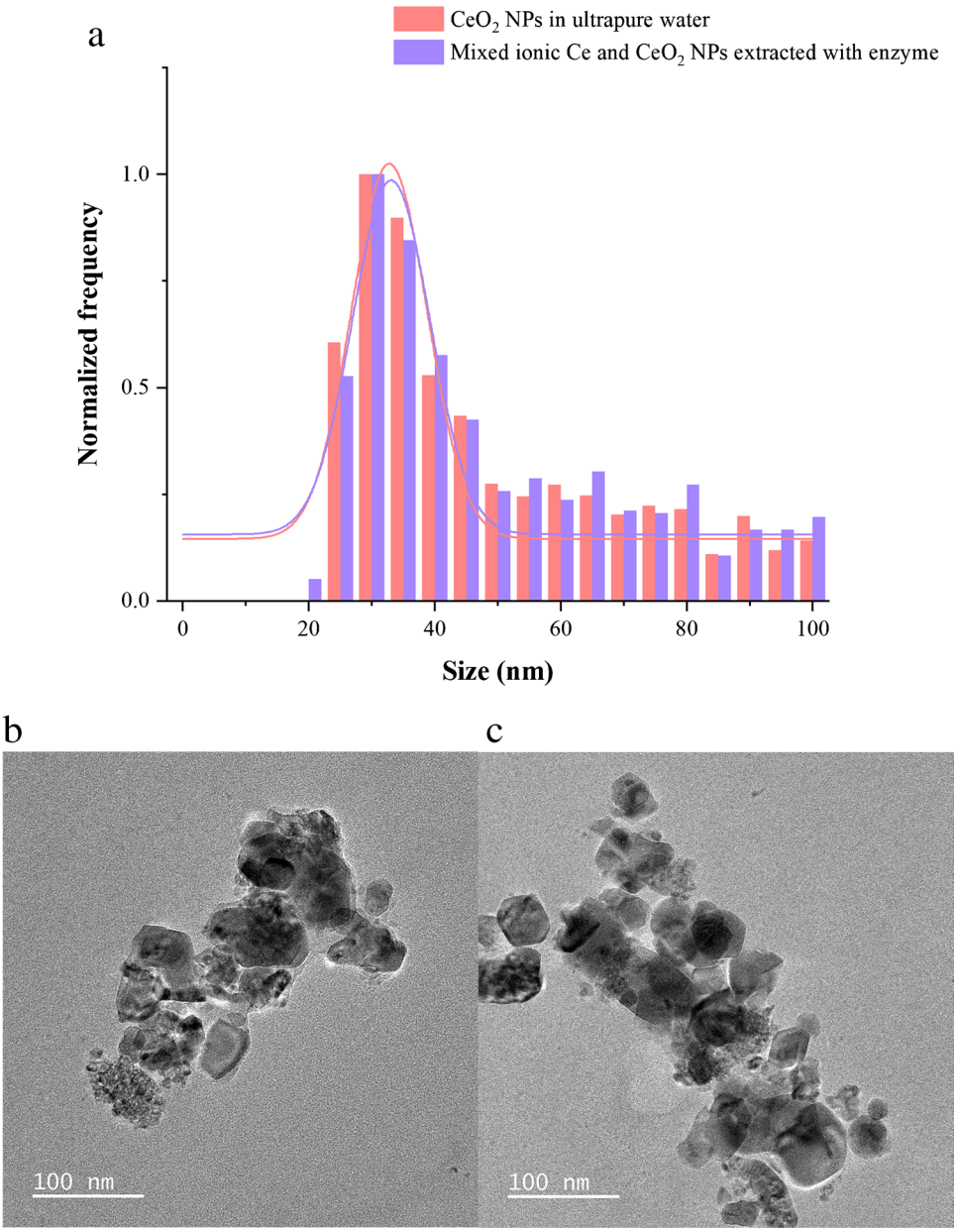

Fig. 3 Characterization of CeO_2 NPs in ultrapure water and in enzyme-pretreated matrix in the case of ionic Ce and CeO_2 NPs mixture. **a** Size distribution obtained by sp-ICP-MS; **b** TEM image of CeO_2 NPs in ultrapure water; **c** TEM image of CeO_2 NPs after enzymatic pretreatment

This is the first study to evaluate the impact of enzymatic and alkaline sample pretreatment on Ce species (both ionic and nanoparticulate Ce species). In previous studies, only the impacts of the sample pretreatment methods on NPs have been investigated [17, 19, 32], while the ionic species, which might dissolve from the NPs in the biological system, were neglected. The lack in analytical technique hinders the in-depth investigation of CeO_2 NP biotransformation. However, the integrated ICP-MS-based analytical approach with enzymatic pretreatment developed in this study shows satisfactory analytical performance in fractionation and characterization of Ce species. In the spiking experiment, both Ce species and CeO_2 NP morphology were well preserved during the sample preparation process with enzymatic pretreatment, and thus any changes of Ce species or NP size measured with this analytical approach would be regarded as the in vivo biotransformation of CeO_2 NPs after their release from animal tissues in the following study. This analytical approach enables us to investigate the in vivo dissolution and size transformation of CeO_2 NPs, and hence provides potential insights into the mechanism of biotransformation.

Bioaccumulation and biotransformation of Ce in mice over time

Figures 4 and 5 show the bioaccumulation of Ce (both nanoparticulate and ionic Ce) in thymus, spleen, liver, and kidney after intraperitoneal administration. The concentrations of Ce in the tested organs of the NP-treated groups were significantly greater than those of the vehicle control groups, with the concentrations of Ce below the limit of quantification. Figures 6 and 7 show the size distribution and particle number concentration of CeO_2 NPs. CeO_2 NPs spiked in enzyme-pretreated solution are regarded as pristine NPs in the following discussion.

In our 90-day study, the highest concentration of Ce was found in the thymus (Fig. 4a). After the single intraperitoneal injection, the concentration of total Ce in the thymus was increased significantly on day 1 and showed continued increase on day 7. However, on day 28, the Ce concentration

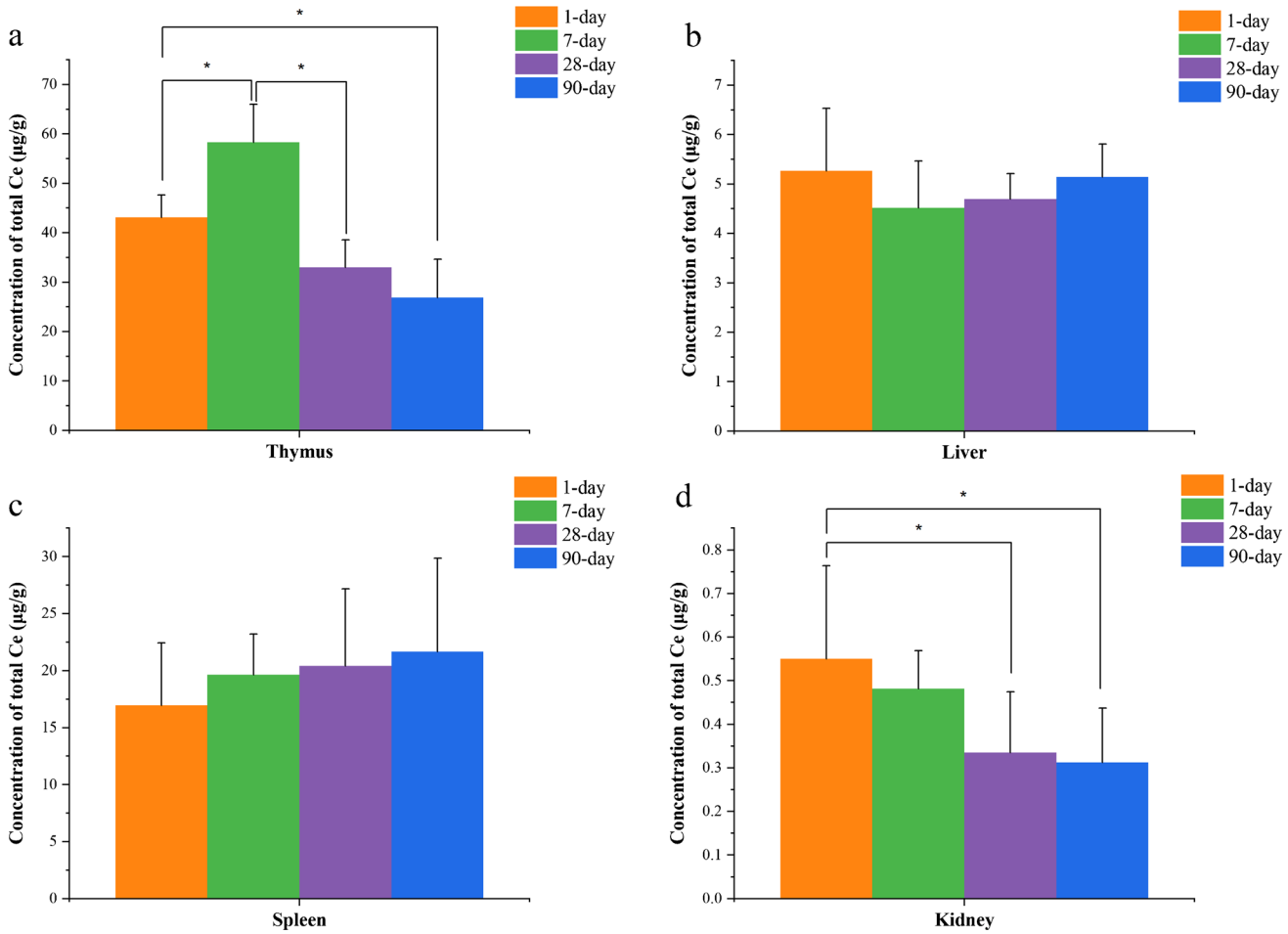

Fig. 4 Concentrations of total Ce measured with conventional ICP-MS in **a** thymus; **b** liver; **c** spleen; **d** kidney ($n=5$)

dropped significantly and remained at a similar level until day 90. It is believed that the prolonged, continuous increase of Ce concentration in the first week after exposure was caused by the way of administration — in the case of intraperitoneal administration, the NPs are taken up primarily by peritoneal macrophages in the abdomen, which then migrate to the thymus [36, 37]. During the first week post-exposure, the macrophages carrying Ce translocated slowly from the peritoneum to thymus [36], and then the macrophages entered the lymphatic system through lymph vessels, leading to the decrease of Ce in thymus after day 7. However, on day 28, no obvious increase of total Ce concentration was observed in the tested organs, especially in the spleen, which plays an important role in lymphatic circulation. We infer that the Ce translocated to the parathymic lymph nodes [37, 38]. In terms of the change of total Ce concentration, the thymus can be regarded as the "holding station" for in vivo NP translocation. Furthermore, the concentration of ionic Ce was quite low (< 0.5 μg/g) (Fig. 5a); ionic Ce accounted for only < 2% of total Ce (data not shown) in thymus. The size of CeO_2 NPs did not change much compared with the pristine NPs (Fig. 6a). Gaussian fitted curves representing the CeO_2 NP size distributions of the 1-day, 7-day, 28-day, and 90-day post-exposure groups overlapped, indicating the median diameter remained ~ 30 nm over time (Fig. 6b). The mass recoveries of NPs extracted from thymus in sp-ICP-MS analysis were all above 80% in all the NP-treated groups, illustrating that over 80% of the NPs can be detected by sp-ICP-MS (Table 5). These results suggest that CeO_2 NPs barely changed in size after they translocated to thymus up to 90 days, further supporting the hypothesis that thymus plays the role of "holding station" in CeO_2 NPs' biological fate.

The concentration of total Ce was relatively stable in liver in this 90-day investigation (Fig. 4b), showing no statistical difference among the four NP-treated groups sacrificed on days 1, 7, 28, and 90. However, the dissolved Ce showed the highest concentration on day 1 and decreased to the lowest after 1 week. CeO_2 NPs showed agglomeration on day 1 compared to the pristine NPs (Fig. 6c) and the obvious right skew from day 1 to day 7 suggested

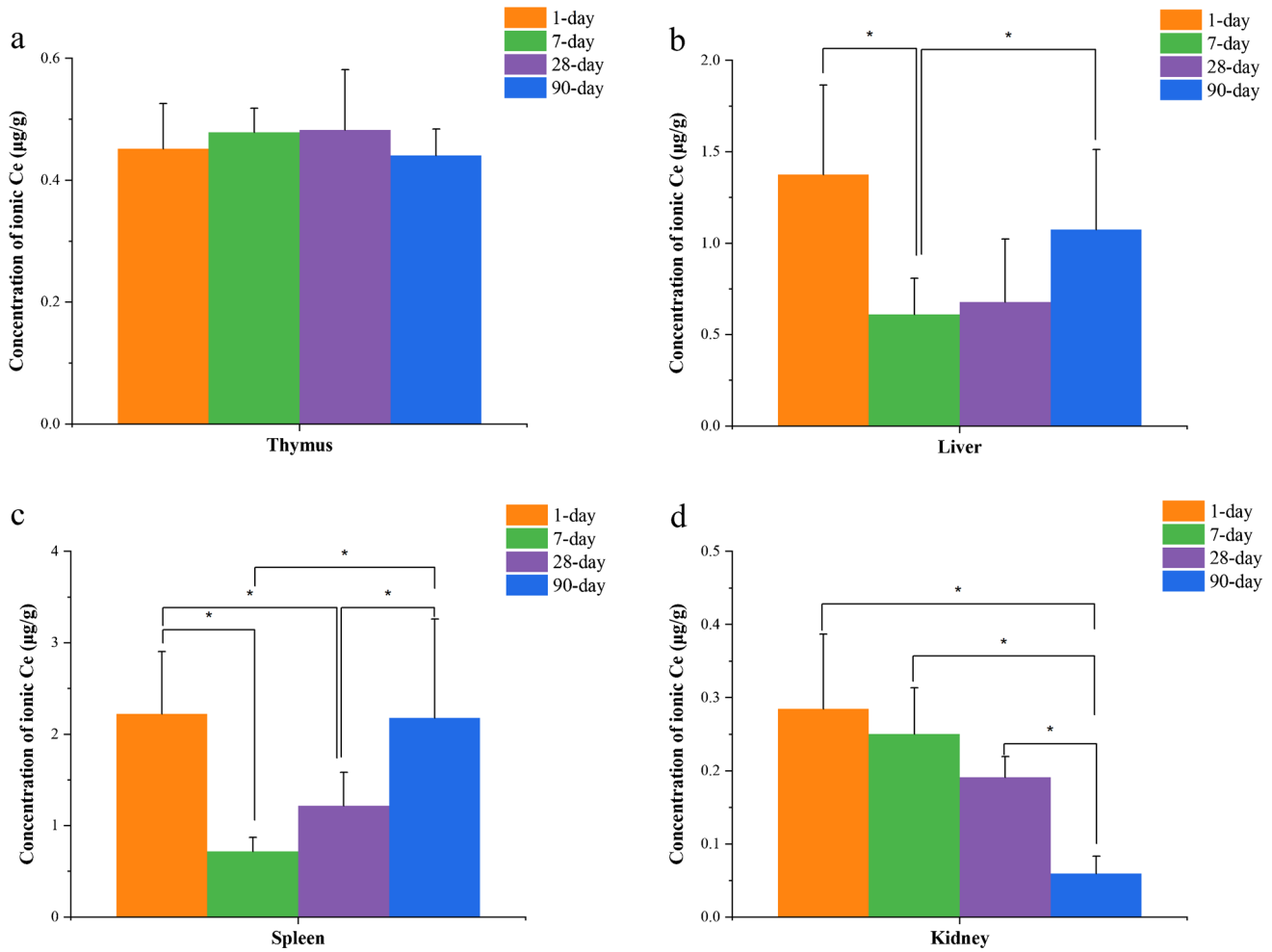

Fig. 5 Concentrations of ionic Ce measured with conventional ICP-MS in **a** thymus; **b** liver; **c** spleen; **d** kidney ($n = 5$)

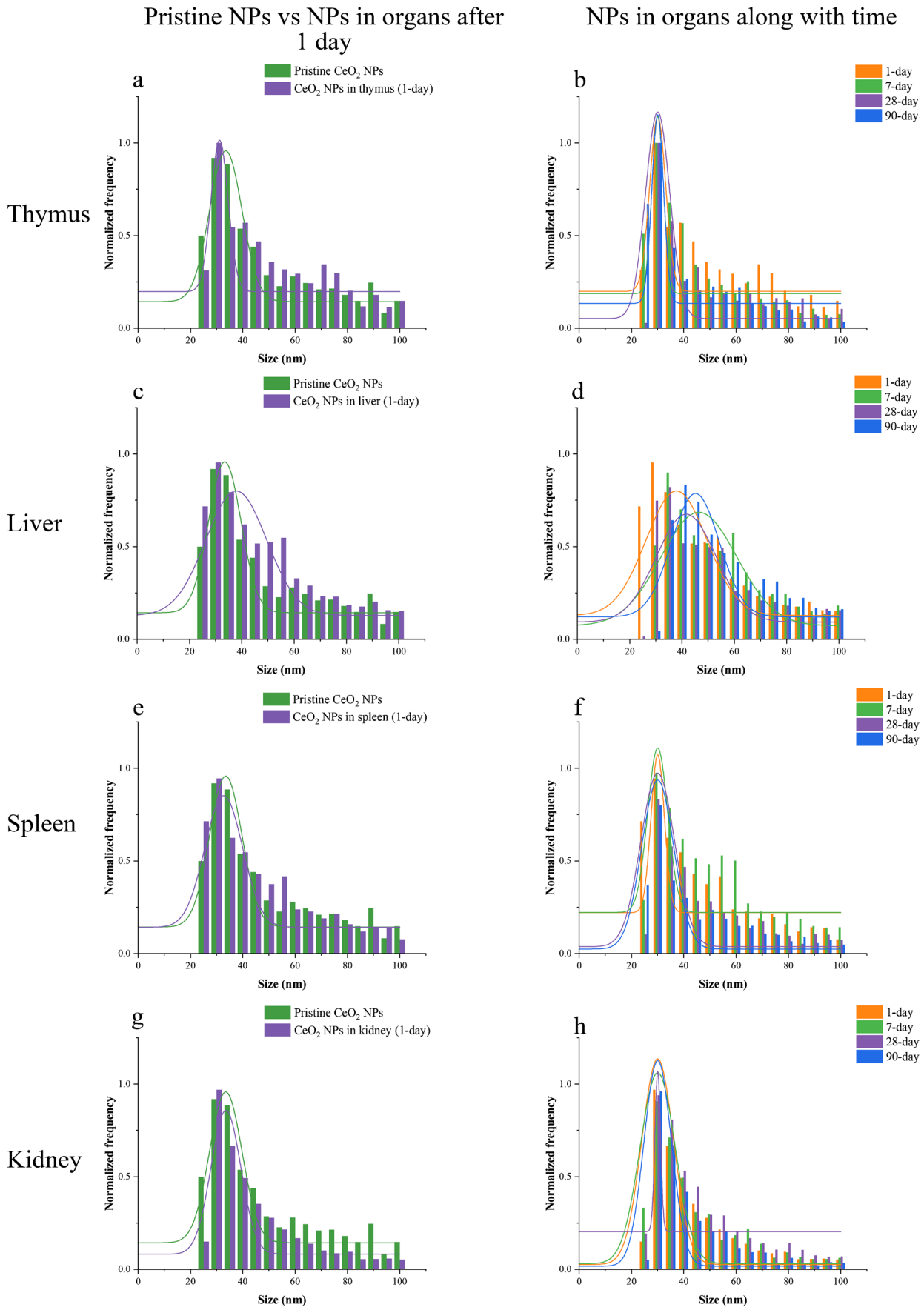
Pristine NPs vs NPs in organs after 1 day
NPs in organs along with time
Thymus
Liver
Spleen
Kidney
a
b
c
d
e
f
g
h
Pristine CeO2 NPs
CeO2 NPs in thymus (1-day)
CeO2 NPs in liver (1-day)
CeO2 NPs in spleen (1-day)
CeO2 NPs in kidney (1-day)
1-day
7-day
28-day
90-day
Normalized frequency
Size (nm)

◂**Fig. 6** Size distributions of CeO_2 NPs detected by sp-ICP-MS. CeO_2 NPs showed minor size transformation in thymus (**a**, **b**), liver (**c**, **d**), spleen (**e**, **f**), and kidney (**g**, **h**) compared with pristine NPs and along with time

the median size of CeO_2 NPs increased in the first week. From day 7 to day 90, the ionic Ce concentration in liver increased, while the size distribution of CeO_2 NPs kept right-skewed, indicated by the rise in the median size from ~ 38 on day 7 to 45 nm on day 90 (Fig. 6d). These results indicate that ionic Ce was likely to be dissolved from the NPs with smaller diameters (25–30 nm) since the larger surface-to-volume ratio made them more susceptible to the complex environment after their translocation to liver. In the post-exposure days, CeO_2 NPs agglomerated in liver.

In spleen, the ionic Ce followed a similar tendency as in liver. CeO_2 NPs maintained a similar size distribution after they were translocated to spleen on day 1 compared to the pristine NPs (Fig. 6e). In the post-exposure period, the Gaussian fitted curves of CeO_2 NPs showed little change (Fig. 6f). However, in the 90-day post-exposure group, the mass recovery as shown by sp-ICP-MS analysis was significantly lower, implying that ca. 40% of the Ce-containing particulates were smaller than 15 nm, approaching the size LOD in sp-ICP-MS analysis (Table 5). The significant drop of particle number concentration on day 90 (Fig. 7c) also suggested that the particles that can be detected by sp-ICP-MS decreased. In other words, by day 90, CeO_2 NPs were smaller in spleen. Graham et al. [39] have observed ultrafine Ce particulates (< 3 nm) in spleen after a 90-day intravenous exposure to 30 nm cubic CeO_2 NPs through high-resolution TEM.

In kidney, the Ce and ionic Ce concentrations consistently decreased during the 90-day investigation. The concentrations of CeO_2 NPs of the four time point groups, obtained by subtracting ionic Ce concentration from total Ce concentration, showed no significant difference among groups (data not shown), indicating that the dissolved Ce was excreted from kidney. According to Molina et al. [40], the ionic Ce in kidney was excreted in urine. In terms of CeO_2 NPs, an obvious decrease in normalized frequency of NPs with 25 nm was observed on day 1 compared to pristine NPs (Fig. 6g), and the median diameters of CeO_2 NPs

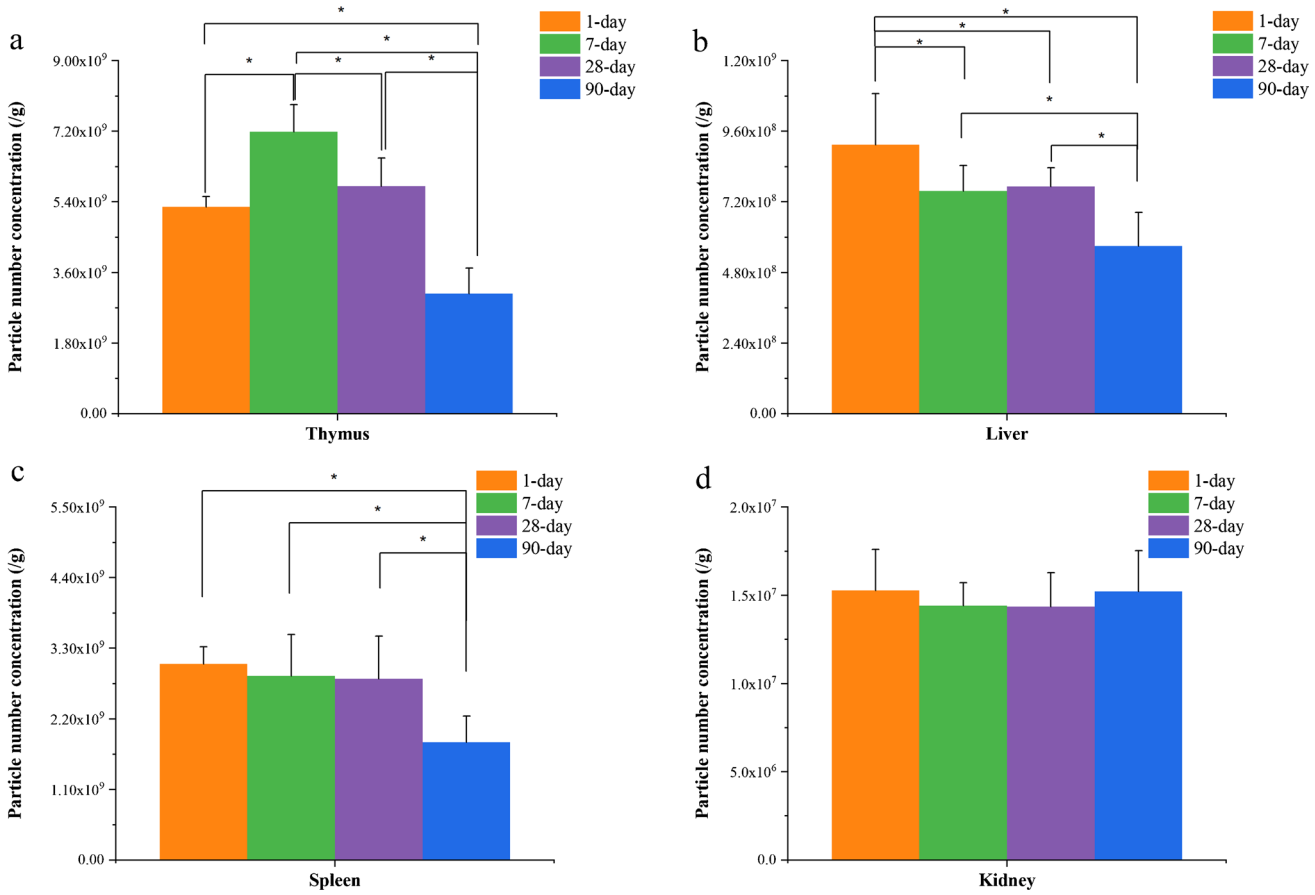

Fig. 7 Particle number concentrations of CeO_2 NPs in **a** thymus; **b** liver; **c** spleen; and **d** kidney ($n = 5$)

Table 5 Mass recoveries of NPs in sp-ICP-MS ($n = 5$)

	1-day (%)	7-day (%)	28-day (%)	90-day (%)
Thymus	89.7 ± 10.3	91.5 ± 12.5	88.7 ± 12.1	81.9 ± 6.3
Liver	97.9 ± 12.3	87.9 ± 17.2	86.0 ± 6.7	83.2 ± 5.8
Spleen	95.3 ± 18.2	78.9 ± 3.5	83.2 ± 4.9	58.6 ± 11.2*
Kidney	93.4 ± 17.7	96.4 ± 10.8	97.5 ± 11.5	97.2 ± 12.3

were ~ 30 nm in the following days (Fig. 6h). In addition, the particle number concentrations of CeO_2 NPs showed no statistical difference during the post-exposure (Fig. 7d). In other words, CeO_2 NPs with 25 nm diameter dissolved in kidney on day 1. These results suggested that dissolution of CeO_2 NPs took place once they translocated to the kidney within the first day. In the following days, dissolved Ce probably was excreted from kidney in urine, while the rest of CeO_2 NPs were retained in the kidney and their biotransformation seemed to be minor.

In summary, thymus is shown to be a "holding station" in CeO_2 NP translocation in mice. The biotransformation of CeO_2 NPs is organ-specific. In addition, the dissolution of CeO_2 NPs in spleen and liver was prominent, indicating that it cannot be neglected when conducting in vivo investigation of CeO_2 NPs.

Conclusion

In this study, we firstly compared the effect of alkaline and enzymatic pretreatment on ionic Ce and CeO_2 NPs during the release of Ce species from animal tissues. Our study showed that, after alkaline pretreatment, ionic Ce formed precipitates in the sample matrix. Worse still, the TMAH-pretreated matrix resulted in increased transport efficiency in sp-ICP-MS analysis, leading to the overestimation of CeO_2 NP mass concentration and particle number concentration. Enzymatic pretreatment resulted in excellent recovery of ionic Ce and CeO_2 NPs without altering their properties after the sample preparation. The performance of this integrated ICP-MS-based analytical approach, in which enzymatic pretreatment is used to release Ce species from animal tissues and multistep analysis is applied to fractionate, quantify, and characterize Ce species, was evaluated using lyophilized tissue spiked with a mixture of ionic and nanoparticulate Ce. The satisfactory recoveries and the comparable size distribution of CeO_2 after enzymatic pretreatment and that of primary CeO_2 NPs demonstrated the competence of this ICP-MS-based approach in quantifying and characterizing ionic and nanoparticulate Ce species. We then applied this integrated approach to investigate the bioaccumulation and biotransformation of CeO_2 NPs in mice after the single intraperitoneal administration. It was found that CeO_2 NP biotransformation is organ-specific, and thymus is likely to be a "holding station" during the in vivo translocation of CeO_2 NPs. The success of the integrated ICP-MS-based analytical approach in analyzing CeO_2 NP in vivo biotransformation highlights its potential in analyzing NP dissolution or size transformation in biological matrices. With this powerful analytical approach to characterize the transformed species after NP biotransformation, the mechanism of biotransformation can be better understood.

Supplementary Information The online version contains supplementary material available at https://doi.org/10.1007/s00216-022-03958-z.

Acknowledgements The authors thank the Hong Kong Research Grants Council (HKBU 12302020 and 12302821) for their financial support. We appreciate Dr. Patrick Y.-K. Yue for his technical support in animal experiments. Y. Huang is supported by a postgraduate studentship offered by the University Grants Committee. The graphical abstract and Fig. 1 were created with BioRender.com.

Author contribution Yingyan Huang: conceptualization; methodology; validation; formal analysis; investigation; data curation; writing — original draft; writing — review and editing.

Judy Tsz-Shan Lum: conceptualization; methodology; writing — review and editing.

Kelvin Sze-Yin Leung: conceptualization; writing — review and editing; supervision; project administration; funding acquisition for Y. Huang.

Declarations

Competing interests The authors declare no competing interests.

References

1. Research GV. Cerium oxide nanoparticles market size, share & trends analysis report by application (energy storage, polishing sgent, personal care, pharmaceuticals), by region, and segment forecasts, 2018–2025. https://www.grandviewresearch.com/industry-analysis/cerium-oxide-nanoparticles-market (Date Accessed 2017 Accessed, date last accessed).
2. Loddo V, Yurdakal S, Parrino F. Economical aspects, toxicity, and environmental fate of cerium oxide. In: Scirè S, Palmisano LS, editors. Cerium oxide (CeO_2): synthesis, properties and applications. Elsevier; 2020. p. 359–73. https://doi.org/10.1016/B978-0-12-815661-2.00009-8.
3. Phalyvong K, Sivry Y, Pauwels H, et al. Occurrence and origins of cerium dioxide and titanium dioxide nanoparticles in the Loire River (France) by single particle ICP-MS and FEG-SEM imaging. Front Environ Sci. 2020;8:141. https://doi.org/10.3389/fenvs.2020.00141.
4. Jreije I, Azimzada A, Hadioui M, et al. Measurement of CeO_2 nanoparticles in natural waters using a high sensitivity, single particle ICP-MS. Molecules. 2020;25(23):5516. https://doi.org/10.3390/molecules25235516.
5. Phalyvong K, Sivry Y, Pauwels H, et al. Assessing CeO_2 and TiO_2 nanoparticle concentrations in the Seine River and its tributaries near Paris. Front Environ Sci. 2021;8:271. https://doi.org/10.3389/fenvs.2020.549896.

6. Yu Y, Li Y, Li B, et al. Metal enrichment and lead isotope analysis for source apportionment in the urban dust and rural surface soil. Environ Pollut. 2016;216:764–72. https://doi.org/10.1016/j.envpol.2016.06.046.
7. Wang L, Han X, Liang T, et al. Discrimination of rare earth element geochemistry and co-occurrence in sediment from Poyang Lake, the largest freshwater lake in China. Chemosphere. 2019;217:851–7. https://doi.org/10.1016/j.chemosphere.2018.11.060.
8. Yessoufou A, Ifon BE, Suanon F, et al. Rare earth and precious elements in the urban sewage sludge and lake surface sediments under anthropogenic influence in the Republic of Benin. Environ Monit Assess. 2017;189(12):625. https://doi.org/10.1007/s10661-017-6331-6.
9. Gambardella C, Gallus L, Gatti AM, et al. Toxicity and transfer of metal oxide nanoparticles from microalgae to sea urchin larvae. Chem Ecol. 2014;30(4):308–16. https://doi.org/10.1080/02757540.2013.873031.
10. Hawthorne J, De la Torre RR, Xing B, et al. Particle-size dependent accumulation and trophic transfer of cerium oxide through a terrestrial food chain. Environ Sci Technol. 2014;48(22):13102–9. https://doi.org/10.1021/es503792f.
11. Cai X, Liu X, Jiang J, et al. Molecular mechanisms, characterization methods, and utilities of nanoparticle biotransformation in nanosafety assessments. Small. 2020;16(36):e1907663. https://doi.org/10.1002/smll.201907663.
12. Yokel RA, Hussain S, Garantziotis S, et al. The Yin: an adverse health perspective of nanoceria: uptake, distribution, accumulation, and mechanisms of its toxicity. Environ Sci Nano. 2014;1(5):406–28. https://doi.org/10.1039/C4EN00039K.
13. Evseeva T, Geras'kin S, Majstrenko T, et al. Comparative estimation of ^{232}Th and stable Ce(III) toxicity and detoxification pathways in freshwater alga Chlorella vulgaris. Chemosphere. 2010;81(10):1320–7. https://doi.org/10.1016/j.chemosphere.2010.08.028.
14. Samal RR, Mishra M, Subudhi U. Differential interaction of cerium chloride with bovine liver catalase: a computational and biophysical study. Chemosphere. 2020;239:124769. https://doi.org/10.1016/j.chemosphere.2019.124769.
15. Mortazavi Milani Z, Charbgoo F, Darroudi M. Impact of physicochemical properties of cerium oxide nanoparticles on their toxicity effects. Ceram Int. 2017;43(17):14572–81. https://doi.org/10.1016/j.ceramint.2017.08.177.
16. Gray EP, Coleman JG, Bednar AJ, et al. Extraction and analysis of silver and gold nanoparticles from biological tissues using single particle inductively coupled plasma mass spectrometry. Environ Sci Technol. 2013;47(24):14315–23. https://doi.org/10.1021/es403558c.
17. Abdolahpur Monikh F, Chupani L, Zuskova E, et al. Method for extraction and quantification of metal-based nanoparticles in biological media: number-based biodistribution and bioconcentration. Environ Sci Technol. 2019;53(2):946–53. https://doi.org/10.1021/acs.est.8b03715.
18. Modrzynska J, Berthing T, Ravn-Haren G, et al. *In vivo*-induced size transformation of cerium oxide nanoparticles in both lung and liver does not affect long-term hepatic accumulation following pulmonary exposure. PLoS ONE. 2018;13(8):e0202477. https://doi.org/10.1371/journal.pone.0202477.
19. Vidmar J, Buerki-Thurnherr T, Loeschner K. Comparison of the suitability of alkaline or enzymatic sample pre-treatment for characterization of silver nanoparticles in human tissue by single particle ICP-MS. J Anal At Spectrom. 2018;33(5):752–61. https://doi.org/10.1039/C7JA00402H.
20. Hadioui M, Leclerc S, Wilkinson KJ. Multimethod quantification of Ag^+ release from nanosilver. Talanta. 2013;105:15–9. https://doi.org/10.1016/j.talanta.2012.11.048.
21. Meermann B, Nischwitz V. ICP-MS for the analysis at the nanoscale—a tutorial review. J Anal At Spectrom. 2018;33(9):1432–68. https://doi.org/10.1039/C8JA00037A.
22. Zhou X-X, Liu J-F, Geng F-L. Determination of metal oxide nanoparticles and their ionic counterparts in environmental waters by size exclusion chromatography coupled to ICP-MS. NanoImpact. 2016;1:13–20. https://doi.org/10.1016/j.impact.2016.02.002.
23. Loosli F, Wang J, Sikder M, et al. Analysis of engineered nanomaterials (Ag, CeO_2 and Fe_2O_3) in spiked surface waters at environmentally relevant particle concentrations. Sci Total Environ. 2020;715:136927. https://doi.org/10.1016/j.scitotenv.2020.136927.
24. Clar JG, Platten WE 3rd, Baumann EJ Jr, et al. Dermal transfer and environmental release of CeO_2 nanoparticles used as UV inhibitors on outdoor surfaces: implications for human and environmental health. Sci Total Environ. 2018;613–614:714–23. https://doi.org/10.1016/j.scitotenv.2017.09.050.
25. Xie C, Zhang J, Ma Y, et al. Bacillus subtilis causes dissolution of ceria nanoparticles at the nano–bio interface. Environ Sci Nano. 2019;6(1):216–23. https://doi.org/10.1039/c8en01002a.
26. Rohder LA, Brandt T, Sigg L, et al. Influence of agglomeration of cerium oxide nanoparticles and speciation of cerium(III) on short term effects to the green algae Chlamydomonas reinhardtii. Aquat Toxicol. 2014;152:121–30. https://doi.org/10.1016/j.aquatox.2014.03.027.
27. Zhang W, Dan Y, Shi H, et al. Elucidating the mechanisms for plant uptake and in-planta speciation of cerium in radish (Raphanus sativus L.) treated with cerium oxide nanoparticles. J Environ Chem Eng. 2017;5(1):572–7. https://doi.org/10.1016/j.jece.2016.12.036.
28. Huang Y. Lum JT-S, Leung KS-Y; Single particle ICP-MS combined with internal standardization for accurate characterization of polydisperse nanoparticles in complex matrices. J Anal At Spectrom. 2020;35(10):2148–55. https://doi.org/10.1039/d0ja00180e.
29. Chen B, Lum JT-S, Huang Y, et al. Integration of sub-organ quantitative imaging LA-ICP-MS and fractionation reveals differences in translocation and transformation of CeO_2 and Ce^{3+} in mice. Anal Chim Acta. 2019;1082:18–29. https://doi.org/10.1016/j.aca.2019.07.044.
30. Animal Welfare Advisory Group Agriculture, Fisheries and Conservation Department. Code of practice care and use of animals for experimental purposes. Hong Kong; 2004.
31. Pace HE, Rogers NJ, Jarolimek C, et al. Determining transport efficiency for the purpose of counting and sizing nanoparticles via single particle inductively coupled plasma mass spectrometry. Anal Chem. 2011;83(24):9361–9. https://doi.org/10.1021/ac201952t.
32. Loeschner K, Brabrand MS, Sloth JJ, et al. Use of alkaline or enzymatic sample pretreatment prior to characterization of gold nanoparticles in animal tissue by single-particle ICPMS. Anal Bioanal Chem. 2014;406(16):3845–51. https://doi.org/10.1007/s00216-013-7431-y.
33. Van der Zande M, Vandebriel RJ, Van Doren E, et al. Distribution, elimination, and toxicity of silver nanoparticles and silver ions in rats after 28-day oral exposure. ACS Nano. 2012;6(8):7427–42. https://doi.org/10.1021/nn302649p.
34. Loula M, Kana A, Mestek O. Non-spectral interferences in single-particle ICP-MS analysis: an underestimated phenomenon. Talanta. 2019;202:565–71. https://doi.org/10.1016/j.talanta.2019.04.073.
35. Kartikawati NA, Safdar R, Lal B, et al. Measurement and correlation of the physical properties of aqueous solutions of ammonium based ionic liquids. J Mol Liq. 2018;253:250–8. https://doi.org/10.1016/j.molliq.2018.01.040.
36. Pavlova OS, Gulyaev MV, Anisimov NV, et al. New aspects of biodistribution of perfluorocarbon rmulsions in rats: thymus

imaging. Appl Magn Reson. 2020;51(12):1625–35. https://doi.org/10.1007/s00723-020-01242-w.
37. Eggli P, Schaffner T, Gerber HA, et al. Accessibility of thymic cortical lymphocytes to particles translocated from the peritoneal cavity to parathymic lymph nodes. Thymus. 1986;8(3):129–39.
38. Moore JE Jr, Bertram CD. Lymphatic dystem flows. Annu Rev Fluid Mech. 2018;50:459–82. https://doi.org/10.1146/annurev-fluid-122316-045259.
39. Graham UM, Yokel RA, Dozier AK, et al. Analytical high-resolution electron microscopy reveals organ-specific nanoceria bioprocessing. Toxicol Pathol. 2018;46(1):47–61. https://doi.org/10.1177/0192623317737254.
40. Molina RM, Konduru NV, Jimenez RJ, et al. Bioavailability, distribution and clearance of tracheally instilled, gavaged or injected cerium dioxide nanoparticles and ionic cerium. Environ Sci Nano. 2014;1(6):561–73. https://doi.org/10.1039/c4en00034j.